WORKPACKAGE REPORT

WP 2 – Science Chamber and Scheme

Grant Agreement number: 250072

Project acronym: ISENSE

Project title: Integrated Quantum Sensors

Funding Scheme: STREP (ICT-FET-Open)

Date of latest version of Annex I against which the assessment will be made: 4. March 2011

Periodic report: **1st** ☐ **2nd** X **3rd** ☐ **4th** ☐

Period covered: **from 1. July 2011 to 30. June 2012**

WP 2- *Science Chamber and Scheme*

Work package leader: CNRS-SYRTE

Introduction

The overall objective of this work package is to establish and optimize the technological steps necessary to realize a guided atomic quantum sensor, in which atoms are either trapped in optical lattices or levitate thanks to sequences of laser pulses. The feasibility of this technology for gravity sensing will be demonstrated, a small scale (< 1liter) vacuum chamber and an adapted low power atom chip developed. The work will be carried out keeping two main constraints into account: the physical principle has to operate in a reduced volume, the chosen species for the technology demonstrator is Rb. In addition we will lay the foundations to broaden the iSense platform to include further species, which are in particular interesting as optical time and frequency standards or for quantum information applications. Particular attention will be devoted on the evaluation of performances of interferometric schemes applied on alkali-earth species in comparison with alkali atoms.

The work package is organised by subdivision in four tasks, which are listed in the table below.

Task-Nr.	Task	Task Leader
2.1	Interferometer scheme	CNRS-SYRTE
2.2	Low power atom chip	UNOTT
2.3	Small scale vacuum chamber	CNRS-IOGS
2.4	Alternative atoms and schemes for future sensors	UNIFI

Summary of progress towards objectives

Task 2.1

- Optimization of the Ramsey type Wannier-Stark (WS) interferometer
- Realization of a symmetric WS interferometer, insensitive to clock-related phase shifts
- Achieved relative sensitivity: $1\ 10^{-5}$ at 1s
- Investigation of systematic shifts in the WS interferometers, related to the trapping lasers, to the Raman laser light shifts, to laser alignments
- QND measurement on atoms trapped in a cavity
- Realisation of a feedback scheme to protect the coherence of an atomic coherent state against noise
- Acceleration measurements close to a dielectric surface
- Identification of sources of noise and systematic errors on g measurements with resonant tunneling in optical lattice with ^{88}Sr.
- Implementation of dual atom interferometry methods for improved immunity from seismic noise in gravity acceleration measurements (demonstration with ^{87}Rb).

Task 2.2

- Optimized current configuration for an integrated quadrupole field
- Tests of wire block winding for the atom chip have been conducted successfully
- Design of the whole magnetic trap assembly completed
- Design of the atom chip to be mounted on top of the structure being finalised

Task 2.3

- Design of the vacuum chamber
- Titanium vacuum chamber produced, based on the design realised at BHAM.

Task 2.4

- 10^7 atoms in the Yb 3D-MOT at a lifetime of about a minute
- Optimized production of bosonic Sr quantum gases
- Characterization of collisional parameters on ground-state Sr isotopes by cross-thermalization measurements.
- Achieved Bose-Einstein condensation of ^{174}Yb, currently typ. $5x10^4$ condensate atoms at T < 0.2 Tc (condensate fraction > 90%).
- Production of Sr_2 ground state molecules
- Laser cooling to quantum degeneracy

Details for each task;

Task 2.1

- ***Realization of gravity measurements with three different schemes*** *(months 1-18)*

(i) Wannier-Stark interferometer scheme

To obtain a measurement free from light shifts, and more generally to any clock-related phase shifts, we have realized a symmetric type WS interferometer, the "accordion" interferometer, combining microwave and Raman pulses. A first π /2 microwave pulse puts the atoms initially in a given well m in a superposition of the two hyperfine states. A subsequent Raman π pulse shifts the two partial wavepackets in opposite directions. After free evolution times of T/2 and T, microwave π pulses reverse internal states. Finally, after a time T/2, a Raman π pulse brings back partial wavepackets in the original well, where they are recombined with a last π /2 microwave pulse. The use of symmetrisation microwave π pulses suppresses the sensitivity of the interferometer to frequency shifts of the hyperfine transition.

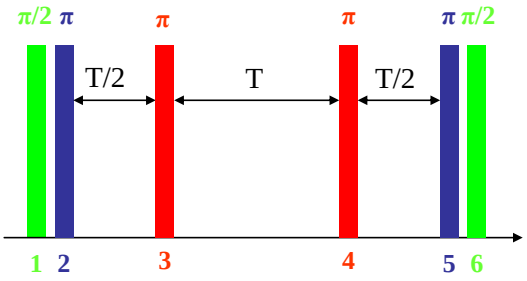

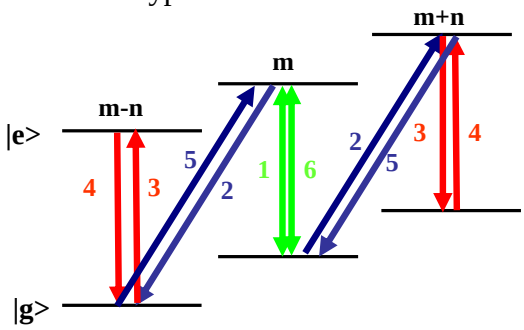

(ii) Modulation scheme

- Acceleration measurements with ^{88}Sr using resonant tunneling via amplitude modulation of optical lattice have been performed close to a dielectric surface.
- Measurement of decoherence rates close to surfaces; found good agreement with a model based on Rayleigh scattering
- Implementation of laser system for dual isotope ^{88}Sr-^{88}Sr trapping in view of differential gravity measurements in the optical lattice

We compared different methods for the accurate determination of forces acting on matter-wave packets in optical lattices [M. G. Tarallo et al., arXiv:1207.2123v1], and investigated in detail the quantum interference nature responsible for the production of both Bloch oscillations (BO) and coherent delocalization. By combining dynamical lattice driving with BO observation in momentum space, we demonstrated a technique for delocalization-enhanced Bloch Oscillations (DEBO, see fig).

By observing the resonant tunneling in an amplitude-modulated (AM) optical lattice up to the sixth harmonic with Fourier-limited linewidth, we measured g with an accuracy of about 2*10^-7 (see fig. 24). We then explored the fundamental and technical phenomena which limit both the sensitivity and the final accuracy of the atomic force sensor at 10^{-7} precision level, with an analysis of the coherence time of the system and addressing few simple setup changes to go beyond the current accuracy.

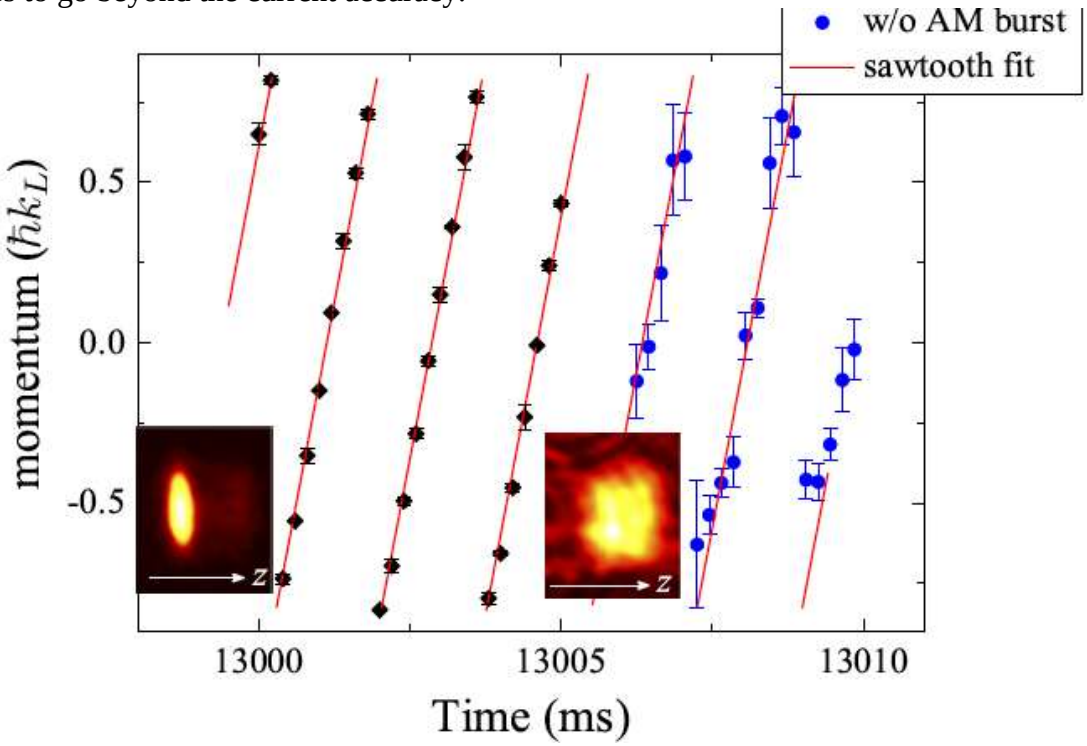

Figure 23: Experimental results of DEBO technique; the plot shows a comparison of Bloch oscillation phase evolution with (black diamonds) and without (blue circles) initial AM burst. In the insets, 2D TOF atomic distributions are displayed for the two cases. The red line is obtained from the best fit with a sawtooth function.

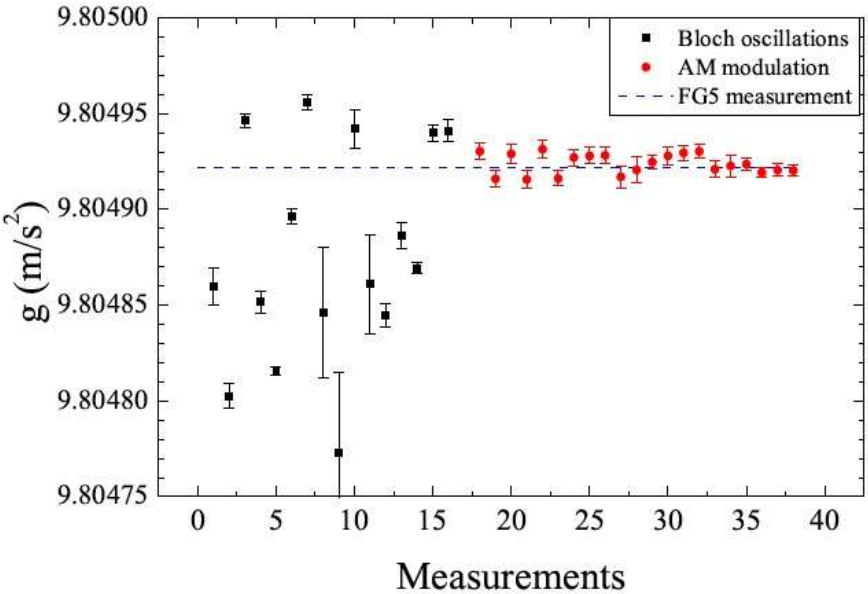

Figure 24: Summary of g measurements with DEBO (black squares) and AM resonant tunneling (red circles).

Main sensitivity limits with BO technique are lattice laser frequency drifts and position

fluctuations in the MOT. We experimentally determined the collisional decoherence time as 530+/-130 s, in agreement with a theoretical estimate based on the atomic density and known scattering length. We also estimated the sensitivity limit due to LZ tunneling do be slightly smaller than 10^-7 g per shot.

Main sensitivity limits with AM resonant tunneling are lattice laser frequency drifts and size fluctuations in the MOT. Typical cloud size fluctuations are around 2%, converting into fluctuations of 370 ppb on g. Another source of decoherence induced by sequential tunneling is given by spurious AM. With an active amplitude control of the lattice laser we keep the RIN below -120 dB in the frequency range between 10 Hz and 100 kHz. This corresponds to a sensitivity limit of 20 ppb on g.

Below the error budget for our absolute g measurement with AM resonant tunneling:

Effect	Correction (10^-7 g)	Uncertainty (10^-7 g)
Lattice wavelength fluctuations	0	2
Lattice beam vertical alignment	0	0.1
Inhom. Stark shift (beam geometry)	14.3 ÷ 17.3	0.4
Experiment timing	0	0.2
Tides	-1.4 ÷ 0.9	<0.1
Off-resonance tunneling	<0.01	0.2

We also investigated the possibility of new gravity tests at micrometer scale. In particular, we performed acceleration measurements with ^{88}Sr using resonant tunneling via amplitude modulation of optical lattice close to a dielectric surface, and we characterized the decoherence rate close to the surface. We found good agreement with a model based on Rayleigh scattering.

In addition, we implemented a laser system for dual isotope ^{87}Sr-^{88}Sr trapping in view of differential gravity measurements in the optical lattice, and implemented the ^{87}Sr trapping.

Finally, we implemented a method for improved immunity from seismic noise in gravity acceleration measurements, based on simultaneous Raman interferometry; the method was demonstrated on a dual-cloud ^{87}Rb interferometer [F. Sorrentino et al., accepted for publication on APL].

(iii) Levitation scheme

We have implemented and optimized the non-demolition detection of the number difference between the hyperfine states of ^{87}Rb. For that purpose, we first implemented a compensation scheme for the differential light shift due to the dipole trap at 1560 nm on ^{87}Rb atoms. The scheme uses a second laser at 1529 nm (on the blue of the P-D transition) injected on the same cavity mode to give an optimal overlap between the two laser sources. The laser is stabilized to the resonator with an original locking scheme that we reported on Optics Letters, based on serrodyne frequency shifting. The principle of the non-destructive measurement of J_z relies on a heterodyne measurement, using a carrier modulated at high frequency (3.6 GHz), with a scheme that compensates for the light shift induced by the probe. Non-

demolition measurements on trapped atomic samples have been demonstrated, thanks to the differential light shift compensation. Continuous measurement of the LO phase have then been performed using a coherent spin state and successive weak, non-demolition detection pulses on the atomic ensemble.

This QND measurement was then used to realize a feedback scheme to protect the coherence of an atomic coherent state against noise, using non-projective weak measurements and retro-action. The results have been recently submitted for publication (see ArXiv: 1207.3203). We are also working to upgrade the detection system to achieve the strongly projective regime (sub-shot-noise), so as to have the possibility to generate spin squeezed ensembles. The main upgrades are:

- the reduction of the beam waist of the detection beam, to increase coupling between the probe and the atoms
- the increase the power of the microwave used to manipulate the atomic spin vector on the Bloch sphere
- the improvement of the feedback electronics
- the substitution of the probe laser, to avoid the technical noise of the ECDL currently adopted

- ***Identification and reduction of sources of instability as well as identification and modelling of systematic errors*** *(months 18-24)*

The sensitivity of the Ramsey type WS interferometer has been optimized. The contrast of the interferometer was found to be limited by the inhomogeneity in the differential light shift from the Raman lasers, which is comparable to the Rabi frequency of the Raman pulses. We obtained at best a relative sensitivity on the measurement of the Bloch frequency of $2\ 10^{-5}$ at 1s measurement time. The sensitivity is found to be limited by detection noise and light shifts fluctuations.

With the accordion interferometer, we achieved a relative sensitivity of $1\ 10^{-5}$ at 1s, thanks to the factor 2 gain in the vertical separation between the partial wavepackets. This sensitivity is still relatively low due to the small spatial separation between the partial wavepackets (of a few µm compared to typical separations of order of several hundred µm in free-falling interferometer). In order to improve the contrast of the interferometer, and to potentially realize sequences of pulses in order to increase this separation, we have tried to implement an adiabatic passage scheme to increase the efficiency of the WS transitions. But we could not improve the efficiency of the transfer to better than 80%. The reasons for this limitation are still under study.

Systematic shifts related to the trapping lasers, to the Raman laser light shifts, to laser alignments have been investigated. In particular, a numerical model of the "accordion" interferometer has been realized. We have calculated the influence of the differential light shift of the Raman lasers on the asymmetry of the fringe pattern. The resulting impact on the determination of the position of the fringe is found to be 5 mHz/Hz of light shift, which agrees with the measurements. We have measured relative bias on the Bloch frequency of a few parts in 10^5 with respect to the expected value. This bias could be explained by the parasitic force due to the gradient of the IR laser, if atoms are not trapped at its waist. The effect was calculated to be as large as $3\ 10^{-6}$/mm of offset with respect to the position of the waist. Measurements of the Bloch frequency versus IR laser intensity and waist position were

performed but were found not reproducible. In addition, we found a non-linear behaviour with laser intensity which we presently cannot explain. A model of this accordion interferometer has also been realized close to the surface of a reflecting material (Pélisson *et al*, Phys. Rev. A 86, 013614 (2012)), indicating that large contrasts can be achieved, both close and far from the surface, using if necessary two simultaneous Raman lasers frequency differences.

- ***Comparison between the different schemes*** *(month 24).*

The comparison and decision upon different schemes was accelerated as compared to the original plan, in order to allow final decisions on laser and vacuum systems to be taken in time and to avoid unnecessary delays in production. We have held a workshop on March 22nd and 23rd in Paris for this purpose. So far the different schemes investigated in iSense have demonstrated sensitivities of 10^{-5} at 1s at best. Even though there is still some room left for improvement, by at least an order of magnitude, it is unlikely that any of the proposed schemes will meet the objectives of the project within the timescale of the project. It was recently demonstrated in *Charrière et al, PRA 85 013639 (2012)* that combining a standard Ramsey Bordé interferometer with Bloch oscillations that prevent atoms from falling allows reaching better performances, while keeping the interrogation volume very small. The demonstrated relative sensitivity, equivalent to 3.10^{-6} at 1s, was limited by detection noise, and can easily be significantly improved with a careful design of the detection system.

In view of the above and the relative simplicity we have decided to choose the scheme of Charriere et al. as the baseline for the demonstrator. We also decided to keep the design sufficiently flexible to allow implementation of any of the other schemes, in case progress is faster than currently anticipated.

Task 2.2

- ***Layout of low power chip design and support structure*** *(months 1-12)*

Layout of a chip design with power consumption below 1W and no external coil requirement. This design will focus on providing a number of microwire based magnetic traps, optimized for fast and efficient loading and cooling of more than 10^7 Rb atoms and transfer of more than 10^4 atoms to optical lattices used in the sensor. Design of a chip support structure fitting in a volume of 100 cm^3 and weighing below 500g when fitted with the chip. This structure will encompass a replaceable header structure that will be directly attached to the atom chip, an integrated larger (millimetre sized) copper trapping structure and broad current sheets for generating homogeneous fields for both chip based and support structure based magnetic traps.

Based on the demonstration of a low-power, but high current chip structure it was decided to make a design iteration in order to optimise the entire power consumption including the current source, which requires lower current and higher voltage operation for efficiency. In view of the developments in the vacuum design and scheme considerations, the following constraints were imposed on a new conductor structure: the zero of the quadrupole field is to be produced 5 mm away from the surface of a chip to be mounted on top of the wires/coils, the field gradient should be 10G/cm along the strong axis, the current used should not exceed 10A, the power dissipation should stay under 10W. Furthermore, the setup has to be compatible with the vacuum chamber, i.e. be mounted on a cf63 flange and its height from inner flange surface to chip surface should be 70mm.

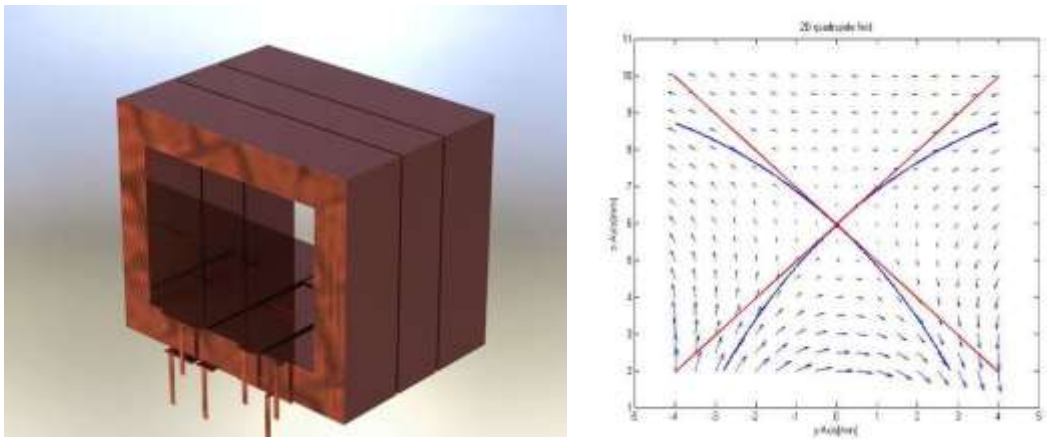

Figure 25: Left, mechanical desing of the wire block. Right, simulation of the magnetig field generated by the wire structure proposed.

The three-wire structure then has to have a wire-wire spacing of ~6mm (5mm+1mm for the chip on the surface), the assembly producing a two- dimensional quadrupole field is shown here, together with the field produced.
The quality of the field (in particular the angular deviation of the quadrupole axes [blue] from the ideal ones [red]) is similar to the working first-generation patterns.
Tests of wire block winding have been conducted successfully (see picture below).

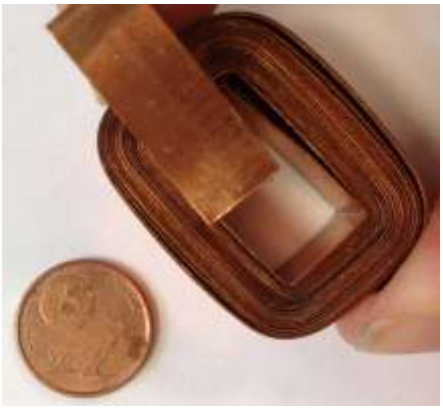

Figure 26: Wire block test realization.

The third dimension requires additional confinement, which in the model is provided by an interlaced UH vacuum compatible PCB (see figure 27). The total three-dimensional quadrupole field calculation again shows similarly low angular deviations from the ideal field as the working first-generation model.

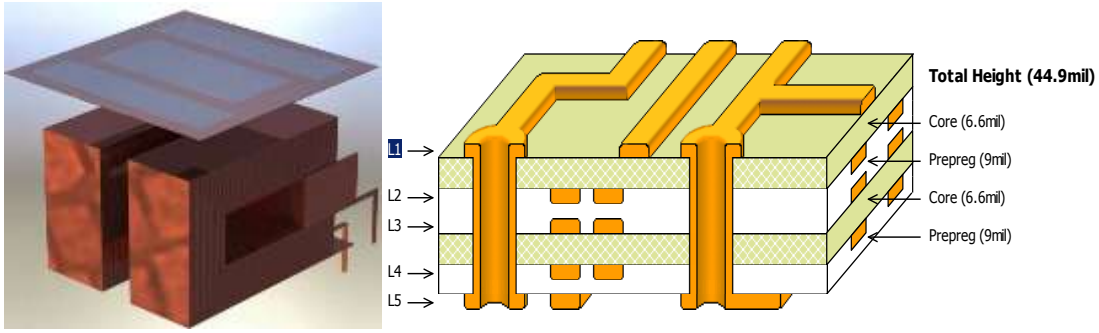

Figure 27: Left, CAD drawing showing overall layout of the atom chip with the microstructured chip-PCB. Righ: scheme of the microstrucutred chip-PCB

- ***Experimental test and optimisation of the full combined assembly*** *(months 12-24).*

A dedicated test ultra-high vacuum apparatus will be constructed to house the atom chip mounted on its support structure including rubidium dispensers as an atom source. A gold surface atom chip will be used as a mirror for magneto-optical trapping and cooling of 10^7 atoms to temperatures below 20 μK a few millimetres away from the chip surface in less than 1s. The necessary magnetic quadrupole field will be provided exclusively by the support structure with a power requirement below 1W. This will facilitate trap compactness, alignment, integration and low power consumption.

The design of the whole assembly has now been completed, the PCB stack is being manufactured externally, the copper structures are machined locally in the UoN workshop. The assembly of all components will be completed within the next two months (until October 2012). The design of the atom chip to be mounted on top of the structure is currently being finalised: it will contain a three Z-shaped wires of several hundred microns width to carry currents of several amps, so that magnetic traps for large atom clouds can be formed away from the surface. While not a direct requirement in iSense, this option would allow for cooling of the samples below laser cooling temperatures for better performance of the prototype gravity sensor. We are planning to produce thick (>10micron) electroplated reflecting Au layers to support large magnetic fields and hence trap volumes. A fallback is a chip with a thermally evaporated Au layer, if necessary w/o lithographic structuring. The design of the whole assembly with vacuum flange and feedthrough is shown below:

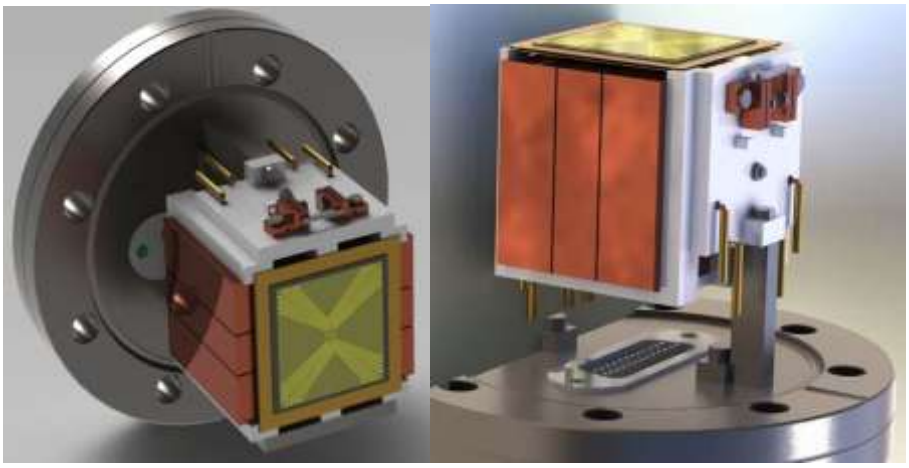

Once the whole block including flange, connections, ceramics holders, copper structures, PCB, and chip is assembled, it will be introduced into a test vacuum chamber to verify UHV compatibility. Once this test is successful, an existing and operational standard laser system for laser cooling of Rb-87 will be used to establish and characterise a MOT. These tests are scheduled for autumn 2012; they are expected to be completed in 2012.

Task 2.3

- ***Investigation of the mechanical interface between vacuum chamber and optical/magnetic components*** *(months 1-24)*

For the interface between vacuum chamber and laser delivery system we have designed a series of fibre collimators aiming for compactness without compromising the laser beam quality required for the experiments to be performed. For this purpose we have designed

three different types of collimators, one for the delivery of the trapping and cooling light, one for the delivery of the interrogation light and one for the delivery of the detection light.

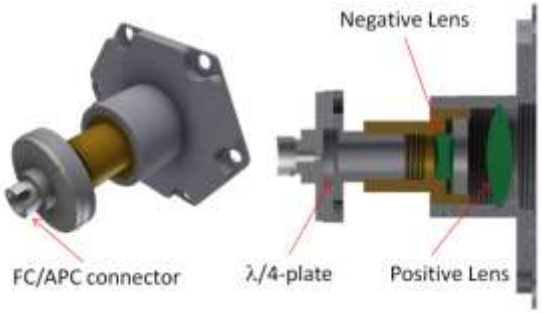

Figure 27: Basic fibre output collimator. They will be built out of Brass and Aluminium to avoid any magnetic field/field gradient in the vicinity of the interrogation volume.

The main difference between the three being the beam size delivered. The beam waists being 4.5mm for the interrogation[1], 10mm for the trapping light and 15mm for the detection light. The collimator will be fixed to the vacuum chamber using the tapered holes used during the sealing of the chamber for compressing the glass windows to the indium rings (see below section "*Construction and test of science/vacuum chamber").*

- ***Investigation of pumping strategies (months 12-24).***

After evaluating the vacuum requirements of the system, and trying to minimize the volume and weight of the pumping system, we have decided that it will consist of a commercial system (SAES Getters SpA, NEXTorr® D100-5). This pump integrates a 100l/s Non-Evaporable-Getter pump plus a 6l/s Ion-Getter-Pump. The system is mounted on a DN35CF flange and has a weight of 2.2kg (including magnets).

- ***Concurrent vacuum/science chamber design v1 (month 18-24).***

We have developed a titanium vacuum chamber with two main regions. The first one, on the top, allows the inset of an atom chip mounted on a DN63CF flange from the back while allowing maximum optical access from the front and has side windows every 45degrees (being all windows set at slight angles with respect to the direction of light). The second one, on the bottom, allows the connection to the pumping section on the back, through a DN35CF flange and has 4 windows, one of them allowing light to propagate in the vertical direction for the interrogation of the atoms in both sections and the other three at 90deg with respect to each other to allow the implementation of different detection schemes.

The inner volume is 0.7 litres and the total volume of the chamber body (ie. not including flanges and pumping section) is 1.7l, giving a net weight of 3.4 kg. The Atom-Chip assembly adds less than 0.2l to the total volume and contributes about 1.2 kg to the total weight. The Pumping section contributes with 0.8l and 3.1kg to the total volume and weight respectively and adds 0.18l to the evacuated volume. Summarizing the vacuum system has an external volume of 3.5l (Taking into account the overall dimension extend up to 13.6l). It has a weight of 8kg. It has an inner, evacuated, volume of 0.9l.

[1] The atoms will be trapped at ~5mm of the atom-chip surface.

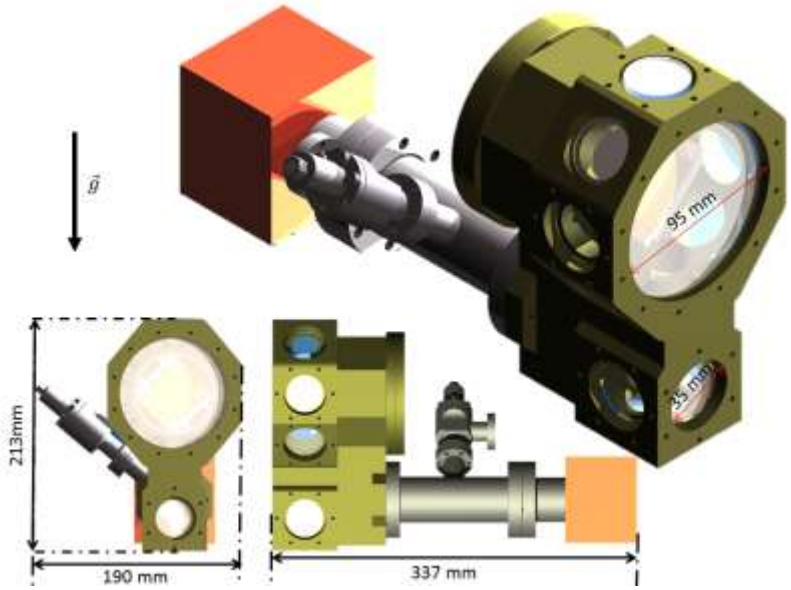

Figure 28: CAD view of the Vacuum Chamber. In green the main chamber with the DN63CF flange holding the atom chip. The red cube represents the NEXTorr© D100-5 pump. The diameter of all windows is 35mm, except for the large front window which has 95mm. In the front and side views the overall sizes are indicated

- ***Construction and test of science/vacuum chamber*** (months 24-27).

The titanium vacuum chamber is being produced at RIAL Vacuum (Parma, Italy), based on the design realised at BHAM. The chamber is realised in a unique block of forged titanium (grade 5, Ti-6Al-4V). The windows are sealed on the chamber using compressed Indium wire. Here the list of the components for the whole prototype setup:

- Nextorr pump D 100-5 (combined ion+getter pump)
- All metal valve to connect the system to the pre-vacuum tee in AISI 316 LN steel
- CVI windows (planarity λ/20 on the Raman beam path, λ/10 otherwise)
- Indium wire compression flanges to place the windows on the chamber using indium.

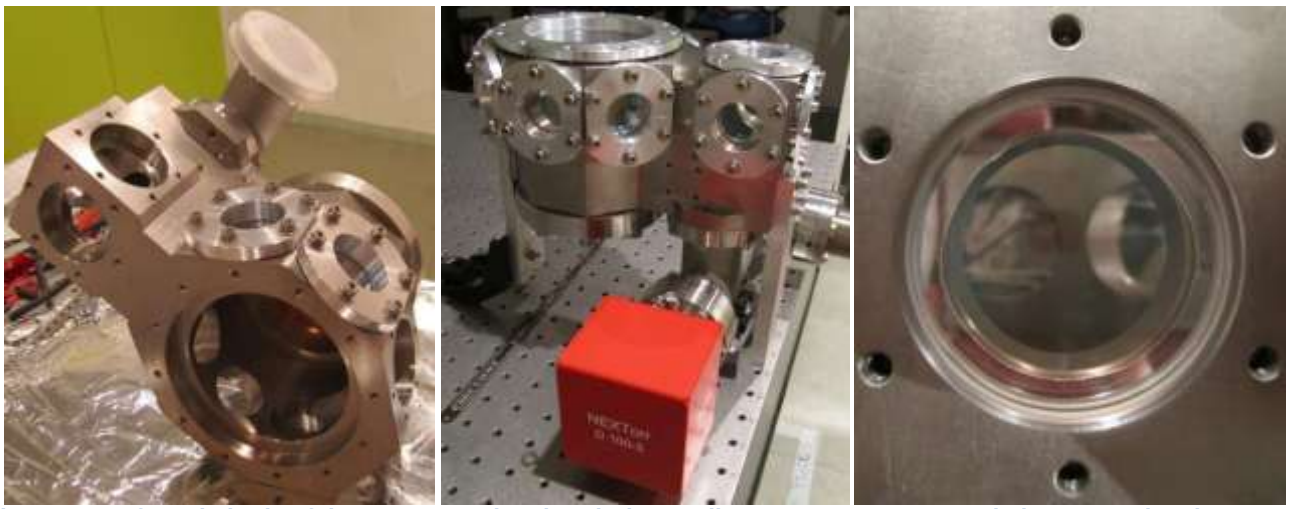

Figure 29: Left: Main body of the Vaccuum Chamber during sealing process. Center, sealed vacuum chamber with NEXTorr© pump attached. Right, detailed view of window sealed with an Indium ring after removing the compression flange.

The vacuum chamber will be closed at the end of August, using a blind flange in place of the atom chip being developed at UNOTT. The flange is provided with three threaded holes to

open the vacuum without mechanically stressing the chamber and especially to preserve the window sealing.

Task 2.4

- ***Demonstration of alkali-earth apparatus*** *(months 1-12)*

UNIFI:

- Implementation of a master-slave scheme for the 689 nm laser source ($^1S_0$-$^3P_1$).
- Implementation of dichroic beam combiners/collimators for dual stage 3D-MOT
- First operation of laser cooling on the $^1S_0$-$^3P_1$ intercombination transition at 689 nm on the transportable apparatus
- Loading of strontium atoms in a vertical optical lattice on the transportable apparatus.

We performed a detailed analysis of collisional properties of ground-state Sr isotopes. Data have been directly acquired on 88Sr and 86Sr, and the parameters for the other isotopes have been derived by mass scaling. More specifically, we have measured the elastic cross sections for both intra-species and inter-species collisions and the three-body inter-species recombination coefficients of 88Sr and 86Sr. The elastic cross sections were determined by driving the system out of thermal equilibrium and measuring the thermalization rate together with the sample density. The inelastic collision rates were extracted from the density dependence of the trap loss rate. The experimental results were compared with theoretical cross sections calculated by standard numerical methods.
The calculated scattering length and its uncertainty is given below in units of the Bohr radius for different isotopic pairs:

88-88: -5(5)
88-86: 95(3)
86-86: 540(80)
84-84: 114(3)
84-86: 24(3)
84-88: 780(180)

These results are in fair agreement with data in literature from photoassociation spectroscopy.

UHH:

Bose-Einstein condensation of Yb has been achieved at UHH as of June 2012 and quasi-pure condensates of about $5x10^4$ atoms of ^{174}Yb have been produced. Currently, preparations for first measurements to verify the ground state and determine the excited state interaction properties of Yb both directly from interaction effects in the condensate and spectroscopically as clock shifts on the ultra-narrow $^1S_0$-$^3P_0$ intercombination transition are in preparation.

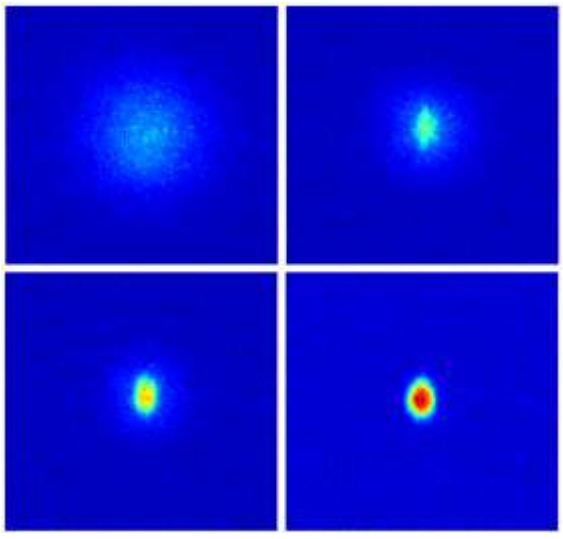

These preparations include improvements on the overall system efficiency and stability to produce larger and longer lived condensates. Work on an

ultrastable laser source for spectroscopy on the cock transition is proceeding well. At this point, a line width of about 100 Hz has been achieved and further reduction is expected soon. Furthermore, cooling of other isotopes than ^{174}Yb, in particular the fermionic isotopes ^{171}Yb and ^{173}Yb, is in preparation.

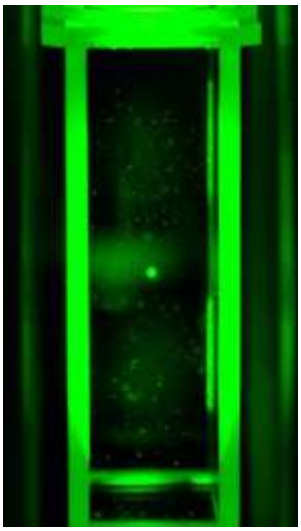

On the road to BEC, we implemented the first two-dimensional MOT for Yb, successfully transferring and adapting this concept of a cold atoms source well known from alkali species, but not yet realized for two-electron atoms with such ultra-low vapour pressures at reasonable temperatures. We successfully demonstrated direct loading of a three-dimensional MOT on the narrow $^1S_0$-$^1P_1$ intercombination transition from the 2D-MOT and implemented pushing and slowing beams yielding a tenfold increase in loading rate with about $5x10^7$ atoms loaded in 15s and less. The temperature in the MOT has been found to be 30µK when producing the first BEC, but has recently been reduced further to about 10 µK. Due to the reduced MOT temperature and hence relaxed constraints on the initial trap depth an increase in condensate size or decrease in cycle time is expected.

For evaporative cooling to quantum degeneracy, a crossed pair of high-power dipole traps has been set up derived from a 532nm solid-state laser. It consists of one tightly focused, horizontal beam of up to 10W laser power, corresponding to trap depths on the order of 1 mK, to load thermal atoms from the MOT and an additional beam of few Watts along the vertical axis to provide tight confinement for efficient evaporation and trapping of the degenerate gas. Initial work to improve the geometry of the trap and evaporative cooling ramps has resulted in a twofold increase in condensate size, a threefold increase in condensate lifetimes, which currently is on the order of several seconds, and a general improvement in stability, e.g. better reproducibility of position and elimination of motion of the condensate. However, further improvements are expected, as the former have been made prior to the reduction in 3D-MOT temperatures reported above.

IQOQI-OEAW:

Optimized production of bosonic Sr quantum gases. Our scheme for the production of large 84Sr BECs, elaborated during Q3 and Q4, has been extended to the other bosonic strontium isotopes. The atom number of ^{86}Sr BECs has been improved to $7x10^4$, a factor 10 increase compared to Q1, and ^{88}Sr BECs now consist of $2x10^5$, a factor four improvement compared to Q1. Furthermore we are now able to produce ^{84}Sr BECs of 10^7 atoms, another factor of 2 improvement compared to Q3. Alternatively we can produce an ^{84}Sr BEC consisting of 10^6 atoms in only 2 seconds. Previously our experimental cycle time was ~15s long. This faster cycle time will be important in the application of Sr quantum gases to precision measurement.

Fermi sea with high quantum degeneracy. We are now able to produce degenerate Fermi seas with 10^5 atoms at a temperature of 0.15 times the Fermi temperature. Previously our best temperature for this atom number was 0.35 times the Fermi temperature.

Fermionic Mott insulator of 87Sr. We have loaded a degenerate Fermi sea of ^{87}Sr into an optical lattice and observed a fermionic Mott-insulator.

Spectroscopy of the 5s5p 3P2 -> 5s5d 3D1,2,3 transitions. We have determined the frequencies of 5s5p 3P2 -> 5s5d 3D1,2,3 transitions, which gives us also the hyperfine

coupling constants of ^{87}Sr in these states. These transitions can be used for example to pump metastable state atoms back to the ground state, or to detect metastable state atoms.

Production of Sr2 ground state molecules. Ultracold molecules have manifold applications in precision measurement, for example in the determination of variations of fundamental constants. Sr_2 molecules are well suited for the model-independent determination of changes in the electron-to-proton mass-ratio. So far, the key step in the efficient creation of ultracold molecules in a well-defined external and internal quantum state has been molecule association using magnetic Feshbach resonances. This magnetoassociation technique cannot be used to form bi-alkaline-earth molecules, because of the lack of magnetic Feshbach resonances in these nonmagnetic species. A similar difficulty arises in the formation of alkali/alkaline-earth molecules, which are predicted to have very narrow Feshbach resonances. The latter molecules would have interesting applications in quantum simulation. We have created ultracold $^{84}Sr_2$ molecules in the electronic ground state. The molecules are formed from atom pairs on sites of an optical lattice using stimulated Raman adiabatic passage. We achieve a transfer efficiency of 30% and obtain 4 x 10^4 molecules with full control over the external and internal quantum state. STIRAP is performed near the narrow $^1S_0$-$^3P_1$ intercombination transition, using a vibrational level of the $1(0_u^+)$ potential as intermediate state. In preparation of our molecule association scheme, we have determined the binding energies of the last vibrational levels of the $1(0_u^+)$, $1(1_u)$ excited-state, and the $X^1\Sigma_g^+$ ground-state potentials.

Laser cooling to quantum degeneracy. We have created Bose-Einstein condensates of strontium by laser cooling. So far, every cooling method capable of reaching BEC in dilute gases relied on evaporative cooling as the last, crucial, cooling stage. Laser cooling to BEC has been strongly discussed middle of the '90s, but the experimental capabilities of that time were insufficient to reach that goal. Strontium's unique properties, especially its narrow intercombination line, allow us a new approach. Laser cooling using this narrow line is able to cool strontium atoms to a temperature below 1 μK and a phase-space density of ~0.1. Further increase of the phase-space density is hindered by reabsorption of photons scattered during laser cooling. We have developed a method with which we can tune the atoms in a small spatial region of a laser cooled sample far out of resonance with the cooling light, overcoming this limitation. To support the sample against gravity, it is held in an optical dipole trap. To increase the density of the gas in the region where it is protected from cooling light, we locally create a deeper dipole potential, into which atoms accumulate by elastic collisions. BECs of 100 thousand atoms are created on a timescale of 100 ms. To demonstrate the cooling power provided by laser cooling, we repeatedly destroy the BEC by locally heating it and observe the formation of a new BEC for more than thirty heating/cooling cycles. It should be possible in a simple way to generalize this new method in order to produce a continuous BEC.

Extension of the Strontium machine to a Rb/Sr double species apparatus.

We have augmented our apparatus with rubidium. This addition required changing the Sr oven and adding a Rb laser system to the machine. The change of the oven gave us an opportunity to take a close look on the strontium distribution inside the old oven after two years of operation, which delivered important insights for future improved oven constructions. After the oven change, we checked that we can still produce Sr BECs and created a first Rb MOT.

- ***Experimental study of collisional parameters of Sr and Yb isotopes*** (months 12-24).

Since writing the iSense proposal many of the intra- and inter-isotope s-wave scattering lengths of both Yb and Sr have been investigated by the international community using spectroscopy and theoretical means: from 2-color PA of various isotops in Yb [PRA 77,

012719], and from 2-color PA and mass scaling [PRA 78, 062708] as well as from Fourier-transform spectroscopy in Sr [PRA 78, 042508].

In Sr, these measurements were obtained in thermal gases. Within iSense UNIFI contributed to the characterization of collisional parameters on ground-state Sr isotopes by cross-thermalization measurements. The performance of evaporative cooling and properties of a degenerate gas can be used to cross-check these calculations experimentally. We did so within iSense by creating BECs and degenerate Fermi gases of all stable isotopes of Sr [PRL 103, 200401; PRA 82, 011608; PRA 82, 041602].

In addition to the "simple" scattering behavior of atoms in the ground state for Sr and Yb, the scattering of two (fermionic) atoms in the excited 3P0 state (and the related case of one atom in the 1S0 ground state and one atom in the 3P0 excited state) are extremely important for the optical clock community and currently investigated by the Ye (Sr), Oates (Yb) and Takahashi (Yb) groups, with theory input from JILA. These groups work with thermal samples of a few μK, and finite temperature (possibly occupation of higher bands) plays a role. The Innsbruck and Hamburg groups have the means to work with really cold and deeply degenerate samples of Sr and Yb respectively, which would provide a much nicer system. We might contribute to this advanced research during the 3rd funding period.

Clearly significant results

Given that none of the schemes have reached the expected performances yet, we have selected a new scheme, recently demonstrated, and compatible with our laser system, which has the advantage of combining Bloch oscillations with a free falling Raman interferometer, allowing for excellent sensitivity while keeping the interrogation volume small.

The designs of the vacuum chamber and of the atom chip assembly have been completed. Their realization is currently underway.

The new molecule creation approach developed at IQOQI widens the range of ultracold molecules that can be created in a fully quantum-state controlled way. This opens new perspectives for precision measurement, especially using Sr2 molecules, but also paves the path towards the creation of RbSr ground-state molecules.

Laser cooling to quantum degeneracy has applications in the fast production of samples of ultracold atoms, as is required for precision measurement. Another exciting prospect enabled by variations of our techniques, is the realization of an atom optics circuit element, which converts a thermal beam of atoms into a continuous atom laser, which could be used to build an atom interferometer.

The augmented apparatus will allow us to study alkali/alkaline-earth mixtures and to create alkali/alkaline-earth ground-state molecules. These molecules have not only a strong electric dipole moment, but also a magnetic dipole moment. This property makes them useful for the quantum simulation of spin-lattice models.

Achievement of Yb BEC.

Deviations from Annex I and their impact on other tasks, available resources and planning
NA

Reasons for failing to achieve critical objectives and/or not being on schedule and explain the impact on other tasks as well as on available resources
The delivery of the trap and sensor chip is delayed by 6 months. This delays the final sealing of the vacuum system by 3 months but is not anticipated to have a major impact on the schedule for the integration of the overall system.

Statement on the use of resources, highlighting and explaining deviations between actual and planned person-months per work package and per beneficiary in Annex 1
The use of resources is in general agreement with Annex-I.